



LUND UNIVERSITY
Faculty of Science

Investigation of Aerosol Influence on Operational Weather Forecasts

Nellie Edvardsson

Thesis submitted for the degree of Bachelor of Science
Project duration: 2 months

Supervised by Alexander Mahura and Elna Heimdal Nilsson

Department of Physics
Danish Meteorological Institute
May 2016

Abstract

Low precipitation events are difficult to predict due to the many processes taking part in formation of precipitation. An additional challenge is that many of the processes act on a smaller scale than what weather models can resolve. The aerosol impact on the state of the atmosphere is an example of one of these processes. The aim of this study is to investigate the impact of sea salt aerosols on the prediction of short wave radiation flux, air temperature, and relative humidity, meteorological parameters important for precipitation formation. Including aerosols in weather prediction models might lead to an improvement of weather forecasts.

The numerical weather prediction model HARMONIE is used to complete model runs with and without sea salt aerosols. This is done for two specific cases of low precipitation events, one during winter (7 December 2014) and one during summer (31 May 2015).

Impact of sea salt aerosols on the three meteorological parameters was found, both on the diurnal cycle at the surface and at vertical levels in the atmosphere. For both cases, it was found that the largest impact of sea salt aerosols on air temperature and relative humidity at the surface occurred in connection with low pressure systems present in the area of study. In the vertical, the impact on air temperature was most pronounced in the planetary boundary layer. The difference in relative humidity was strongest at the level of 850-500 hPa. When comparing the two cases, it was found that the impact on short wave radiation flux was more pronounced during summer compared to winter. The impact on air temperature and relative humidity was found to be strongest during the winter.

Acknowledgements

I wish to thank my supervisors Alexander Mahura (Danish Meteorological Institute (DMI), Research and Development Department (RDD)) and Elna Heimdal Nilsson (Lund University, Department of Physics). Alexander for the practical support with the modelling and for providing a good learning environment with constructive discussions and comments throughout my research project. Elna for helpful input on the structure and content of my thesis, and for keeping me on track. I am very grateful to Prof. Sergey Ivanov (Odessa State Environmental University, OSEU) and Dr. Julia Palamarchuk (OSEU) for sharing their knowledge and guiding me through the process of configuring the runs with the HARMONIE NWP model at the High Performance Computer (HPC). Thanks also to Drs. Mats Dahlbom and Martin Sørensen (DMI RDD) for valuable discussions on precipitation radar.

The computer facilities at DMI and the European Centre for Medium-Range Weather Forecast (ECMWF) were used in this study. I would also like to acknowledge the IT Department at DMI, for providing technical support and advices on issues with the high performance computing. Dr. Robert B. Schmunk at NASA provided clarification on the functionality of the data viewer Panoply, used in this research project, for which I am thankful.

The results of this BSc study will be an integral part of annual reporting to ECMWF (expected in June 2016) on the HPC Special Project (2015-2017) EnviroAerosols on ECMWF: "Enviro-HIRLAM/ HARMONIE model research and development for online integrated meteorology-chemistry/aerosols feedbacks and interactions in weather and atmospheric composition forecasting" lead by DMI.

Contents

Abstract	iii
Acknowledgements	v
Abbreviations	viii
1 Introduction	1
2 Background	2
2.1 Aerosols and Weather	2
2.2 Recent Studies on Aerosol Impact	2
3 Methodology	5
3.1 NWP HARMONIE Model	5
3.1.1 Basic Description	5
3.1.2 Numerical Experiment Setup	6
3.1.3 Model Performance	7
3.2 Synoptic Situations for Case Studies	8
3.2.1 Winter Case	8
3.2.2 Summer Case	9
4 Results and Discussion	13
4.1 Analysis for Winter Case	13
4.1.1 Short Wave Radiation	13
4.1.2 Air Temperature	14
Diurnal Cycle	14
Vertical Variability	15
4.1.3 Relative Humidity	18
Diurnal Cycle	18
Vertical Variability	19
4.2 Analysis for Summer Case	22
4.2.1 Short Wave Radiation	22
4.2.2 Air Temperature	23
Diurnal Cycle	23
Vertical Variability	25
4.2.3 Relative Humidity	27
Diurnal Cycle	27
Vertical Variability	29
5 Conclusion and Outlook	31
Bibliography	33

Abbreviations

ALADIN	A ire L imitée A daptation D ynamique I Nitialisation
AROME	A pplications of R esearch to O perations at M Escale
CAPE	C onvective A vailable P otential E nergy
CCN	C loud C ondensation N uclei
DMI	D anmarks M eteorologiske I nstitut (Danish Meteorological Institute)
ECMWF	E uropean C entre for M edium-range W eather F orecasts
GFS	G lobal F orecast S ystem
GRIB	G RIdded B inary
HARMONIE	H irlam A ladin R egional/ M eso-scale O perational N WP I n E uromed
HPC	H igh P erformance C omputer
HIRLAM	H Igh R esolution L ocal A rea M odelling
IN	I ce N uclei
NEA	N orth E uropean A rea
NWP	N umerical W eather P rediction
PBL	P lanetary B oundary L ayer
TKE	T urbulent K inetic E nergy

Chapter 1

Introduction

Weather forecasts are important on an everyday basis for many people. In for example agriculture, a certain weather event can cause large economical damage. In particular, forecasts of precipitation are very important. However, forecasting precipitation is behind prediction of other meteorological parameters due to the many physical processes taking part in the formation of precipitation. These processes also act on very local and small scales, smaller than what is resolved in the weather models of today. The relative humidity is an important factor when predicting precipitation since it is a measure of when the air becomes saturated, which leads to cloud formation. Vertical velocities in turn determine the growth of the droplets which is another important process in precipitation formation. Aerosol particles and their interactions in the atmosphere is a third process affecting precipitation formation and influence atmospheric circulation. By including aerosols in Numerical Weather Prediction (NWP), the prediction of weather parameters and precipitation formation might become more accurate.

The aim of this project is to investigate the impact of sea salt aerosols on numerical weather prediction in the Northern European area. This will be studied using the high resolution, non-hydrostatic HARMONIE NWP model. Model runs will be made with and without sea salt aerosols respectively and for two different cases of low precipitation events, one in winter and one in summer. Low precipitation events are chosen because they tend to be not well predicted and improvement is needed in forecasts of low precipitation events. The meteorological parameters in focus will be incoming solar radiation flux, i.e. short wave radiation flux, air temperature, and relative humidity. The main objective is to study if the prediction of these parameters is improved when including sea salt aerosols in the weather model. The choice of studying one winter and one summer case is made in order to investigate if there is a difference in aerosol impact on weather prediction depending on season.

Chapter 2

Background

2.1 Aerosols and Weather

Aerosols have several impacts on weather and climate, one of them being through the processes of absorbing and scattering solar radiation, referred to as the aerosol direct effect (Boucher et al., 2013). The absorption process leads to local cooling of the air close to the surface due to the decrease in solar radiation reaching the surface, but the net effect is an overall warming of the atmosphere since the upper troposphere is heated due to solar radiation absorption (Andreae et al., 2005). The scattering of solar radiation leads to an overall cooling of the atmosphere since less solar radiation reaches the surface and this local cooling of air spreads throughout the atmosphere through air circulation (Charlson et al., 1992). Scattering aerosols can, for example, be sea salt aerosols, mineral dust, and sulphates. An example of an absorbing aerosol is soot (Andreae et al., 2005).

Besides affecting the climate through scattering and absorption of solar radiation, aerosols have an indirect effect on the climate by acting as Cloud Condensation Nuclei (CCN)(Boucher et al., 2013). A higher number of CCN can lead to increased lifetime of clouds since the high amount of CCN will lead to the cloud droplets not being able to grow large enough to rain out of the cloud (Haywood and Boucher, 2000). When including aerosols in the model simulations, both the direct and indirect effects are taken into account.

Sea salt aerosols, whose impact is studied in this project, are aerosols produced during wave-breaking and they consist of sea salt and organic material present in the ocean (Kristensson and Martinsson, 2015).

2.2 Recent Studies on Aerosol Impact

During the recent decade several studies have found that aerosols have an impact on weather prediction. When aerosols are included in operational weather modelling, the forecasts of certain weather parameters have been shown to become more accurate, to some extent. Results from several such studies are described below.

The focus of the studies done by Toll et al. (2015, 2016) was to investigate the results that are obtained using different datasets of aerosol concentrations in the model runs. In the study from 2016 by Toll et al., three different kind of aerosol datasets were used; two climatological datasets, where one of them was more up to date, and one dataset

with time-varying aerosol concentrations. This study found a rather weak dependence between the forecasted meteorological parameters and which of the datasets that was used. They therefore suggested that the different datasets were similar in their capability to account for the direct effect of aerosols in weather forecasting. When including either of the aerosol data sets in the modelling, the forecasts of temperature, humidity and the simulated radiative fluxes in the lower troposphere was found to become more accurate. Toll et al. (2015) found that aerosol data assimilation and accurate aerosol size distribution are important when modelling forecasts. This study also found that the forecasted temperature came closer to the observed temperature when including aerosols in the model. The domain of both studies by Toll et al. (2015, 2016) was Europe.

Palamarchuk, in collaboration with others (2016, 2015), investigated another aspect of aerosol impact on weather forecasts. The focus of these studies was to research the effect of including different aerosols in model runs during specific cases. Palamarchuk et al. (2015) made model runs with the following sets of aerosols; climatological aerosol concentrations of sea salt, land, organic, and dust aerosols, increased amount of carbon aerosols due to forest fires, only sea salt aerosols, and one run without aerosols. Among other things, the study compared the zero-aerosol run with the run where sea salt, land, organic and dust aerosols were included and looked at short and long wave radiation fluxes, air temperature, specific humidity, vertical velocity, TKE (Turbulent Kinetic Energy) and CAPE (Convective Available Potential Energy). Palamarchuk et al. (2016) compared model runs of an aerosol-free atmosphere with one run including only sea salt aerosols, and one run with sea salt, as well as land, organic and dust aerosols included.

Both studies by Palamarchuk et al. (2016, 2015) concluded that aerosols affect the meteorological parameters through a series of interactions where the aerosols act as a trigger for the interactions. The following steps in the interaction chain is described by Palamarchuk et al. (2016): The aerosols first affect the short- and long-wave radiation fluxes which then alter the vertical profiles of air temperature and humidity. The change in these vertical profiles have a visible effect on cloudiness and precipitation and thereby a change in water content of the atmosphere which in turn has an effect on the short and long wave radiation fluxes.

In a study by Seifert et al. (2012) the aim was to investigate the indirect effect of aerosols when their concentrations on a large-scale had perturbed values. This was researched using a convection-permitting mode in the German NWP model COSMO, and the model runs were made for the summers of 2008, 2009, and 2010. The indirect aerosol impact was studied by running the model with concentrations of CCN and Ice Nuclei (IN) set to high or low values. The parameters in focus of this study were clouds, precipitation, and surface temperature. Seifert et al. (2012) found that the effects of perturbed CCN and IN concentrations on accumulated precipitation were small, and

concluded that this was because the clouds act as a buffering system which leads to the surface precipitation not being affected much by changes in the atmospheric state. The clouds themselves were found to be affected by the CCN and IN concentrations, mainly the amount of water in the clouds, whether they produced rain or snow, and the glaciation of the clouds. The study found a change in near-surface temperature of about ± 0.5 K, but did note that further and more in-depth research needs to be done to confirm this indication in temperature change.

Chapter 3 contains the methodology of this research project. In Chapter 4 the results from the HARMONIE NWP model runs are presented, visualised and analysed, along with discussions of the results. Chapter 5 includes conclusions and a future outlook.

Chapter 3

Methodology

The main research tool of this project is the HARMONIE NWP model, which is being run at the European Centre for Medium-Range Weather Forecasts' (ECMWF) High Performance Computer (HPC). The model is configured to run for a suitable model domain, covering parts of the North Sea, Denmark and southern Sweden, and with some other specific changes, as described in Section 3.1.2. The model runs are made for two cases of low precipitation intensity, 7th of December 2014 (winter case) and 31st of May 2015 (summer case). The model performance of each case is described in Section 3.1.3, where information on difference between model run and observed meteorological data has been collected.

Synoptic descriptions of the two days can be found in Section 3.2. For each event, one reference run is made, with all aerosols included, and one run is made without sea salt aerosols. The meteorological parameters in focus are short wave radiation flux, i.e. incoming solar radiation (with the majority of wavelengths being shorter than $2 \mu\text{m}$), air temperature and relative humidity. The difference between the two runs is computed in every grid point of the domain for every time output of the model (every 3 hours), using MATLAB. The maximum and minimum values of the difference field are computed for each of these time steps and plotted in a graph, in order to look at the variability in the difference between the two runs. This is done for each of the three meteorological parameters. The difference field between the reference run and the run excluding sea salt aerosols is also plotted for each parameter, using the plotting program Panoply, developed by NASA¹.

The analysis for each parameter is made on a diurnal cycle and at different height levels in the atmosphere. The results for the winter and summer case are compared in order to investigate if aerosol impact depends on season.

3.1 NWP HARMONIE Model

3.1.1 Basic Description

The convection permitting Hirlam Aladin Regional/Meso-scale Operational NWP In Euromed (HARMONIE) model is a non-hydrostatic spectral model (Driesenaar, 2009). The model is developed under a cooperation between the ALADIN (Aire Limitée Adaptation

¹Available for download at <http://www.giss.nasa.gov/tools/panoply/>

Dynamique INitialisation) team, Météo-France and the HIRLAM (High Resolution Local Area Modelling) research team (Driesenaar, 2010).

A spectral model is built on a set of mathematical operations which allows one to solve the meteorological equations. The operations are as follows, as described by Krishnamurti et al. (2006): A Fourier transform is applied to the dependent variables of a closed set of the meteorological equations, and thereby a finite expansion of these variables can be made. Using the orthogonal properties of the Fourier functions gives a set of coupled non-linear ordinary differential equations for the coefficients of the functions. These coefficients are functions of time and the vertical coordinate and the equations of the coefficients can be solved by time- and vertical finite-differencing schemes. Summing the functions over a set of chosen finite basis functions and multiplying them by the coefficients then allow for mapping of the solution.

The HARMONIE model has a dynamical core developed by ALADIN which is built on a two-time level semi-implicit Semi-Lagrangian discretisation of the fully elastic equations (Driesenaar, 2009). A Semi-Lagrangian scheme means following individual parcels as in a Lagrangian framework but instead of looking at the total time derivative of a variable, the Lagrangian framework is combined with the Eulerian meaning that a regular grid is used and the partial time derivative, following the motion of the parcel, of the variable is estimated (Kalnay, 2003). In the vertical, the HARMONIE model uses a hybrid coordinate, the same coordinate used in the AROME model (Driesenaar, 2009). This vertical coordinate is a hybrid pressure terrain-following coordinate (Seity et al., 2011).

The parametrisations used in the HARMONIE model are very similar to the ones of the AROME model (Driesenaar, 2009).

3.1.2 Numerical Experiment Setup

In the present study, the stable version 38h1.2 of the HARMONIE model is used, and is run in the research mode. Running the model in the research mode means that the model run will not be completed if, for example, no assimilation can be made due to missing observational data, whereas a model run in the operational mode will be completed even if such an error occurs. The model is configured so that the simulation starts 6 hours before the day of study, i.e. at 18 UTC on the 6th of December 2014 and 30th of May 2015, respectively. The forecast length is set to 30 hours and the output time to every 3 hours. For the number of vertical levels, the default setting of 65 levels is used. The output format is chosen to be GRIdded Binary (GRIB) format, a binary file format used by meteorological institutes to store model data.

The aerosol contribution is included in the model runs using the climate file `sugrida.F90`, which includes all aerosols. In the second model run, this file is configured to exclude sea salt aerosols.

The model domain chosen is the North European Area (NEA) domain which covers a large part of northern Europe, including large open water areas, from which sea salt aerosols originate. The domain is chosen so that the area of study; Denmark, southern Sweden and parts of the North Sea, is at the centre of the domain, as can be seen in Figure 3.1. Figure 3.2 shows a zoomed-in image of the domain, focusing on the area of study.

The NWP model used has a horizontal resolution of 2.5 km and a time step of 50 s. The NEA domain has 1200 grid points along the longitude and 1080 grid points along the latitude. The longitude and latitude of the domain centre is 7°E and 60°N , respectively.



FIGURE 3.1: The North European Area (NEA) model domain.

3.1.3 Model Performance

Every month, the Danish Meteorological Institute (DMI) creates diagrams on how well the weather models they run are performing for different meteorological parameters².

For the winter case, 7th of December 2014, the 24h forecast of the HARMONIE model showed a negative bias of -0.7 K for the air temperature at 2 m. The bias of relative humidity at 2 m was, on average during the entire month of December 2014, about 2-3 % higher than the observed value.

²These verification results and diagrams are available at varulven.dmi.dk/~hirlam/

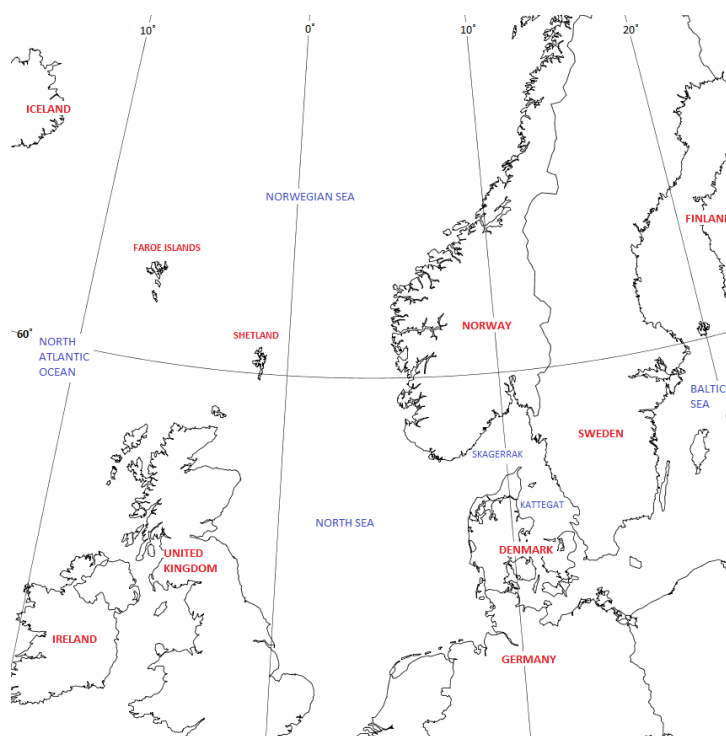


FIGURE 3.2: Area of study.

The 31st of May 2015, the 24h forecast of the air temperature at 2 m showed a negative bias of -0.5 K. The bias of the relative humidity was, on average during the entire month of May 2015, about 4-5 % higher than the observed value.

Following standard verification approach, in both cases, the bias of temperature was calculated by comparing the model result with observational data from synoptic weather stations all over Denmark. Similarly, for relative humidity, the model output and observational data from stations in Denmark are compared. Evaluation showed that overall model performance was good during the two selected cases for both air temperature and relative humidity at 2 m.

3.2 Synoptic Situations for Case Studies

3.2.1 Winter Case

During 6-8th of December 2014, several low pressure systems in the Norwegian Sea dominated the synoptic situation over Denmark and southern Sweden, see Figure 3.3A. A frontal system with a warm front closely followed by a cold front approached the area with the westerly flow. By the time the frontal zone passed southern Sweden and Denmark on the 7th of December it had reached the occluded stage.

On the 6th of December at 18 UTC the westerly wind had a speed of 3 m/s over the land areas of Denmark and southern Sweden, and 8 m/s over the North Sea and the Skagerrak and Kattegat passages (see Figure 3.2 for locations). The air temperature varied about 1-3, 2-6, and 6-8°C in southern Sweden, Denmark, and over the sea, respectively.

The wind speed increased and changed to a north-westerly direction during the night on 7th of December and reached speeds of 8-11 m/s over land and 8-13 m/s over the sea areas at 12 UTC on the 7th. At the same time, the air temperature increased to 2-5°C in Sweden, remained around 6°C in Denmark, and increased to 10°C over the sea. As the front occluded over the North Sea in the afternoon of the 7th of December, the temperature there dropped to 8°C. During the front passage, the wind direction changed from a north-westerly direction to a westerly direction and the wind speed decreased to 10 m/s over the sea area and to 5 m/s over land. After the front passage the temperature was around 0-4°C over land and remained the same over the sea, and the wind kept a steady westerly flow for the next 24 hours.

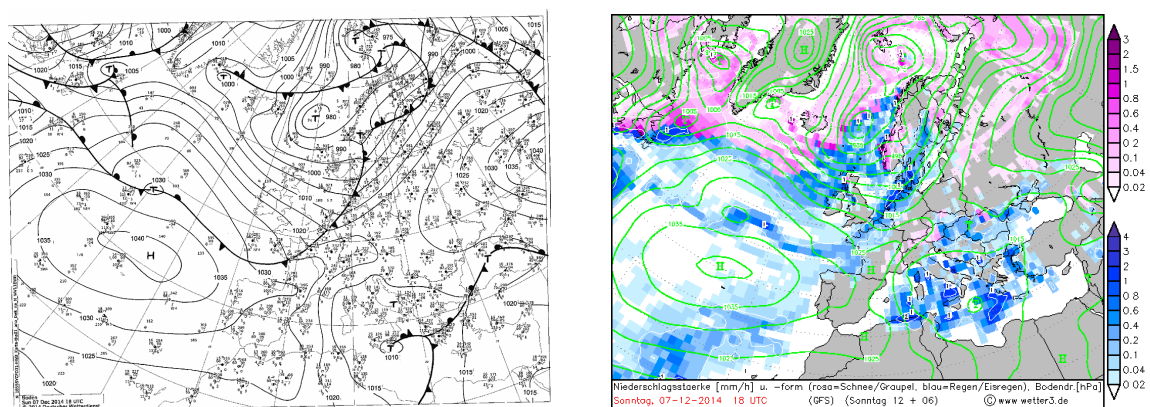
The frontal system brought precipitation into the area of study on December the 7th around 12 UTC. The precipitating area covered Kattegat, Skagerrak, the North Sea, Denmark and parts of southern Sweden. At 18 UTC on the same day the front had moved further to the east and the precipitation occurred over Denmark, southern Sweden and some parts of the sea, as shown in Figure 3.3B. The precipitation was no longer observed over the area during the night on the 8th of December.

The values of air temperature, wind characteristics and precipitation mentioned above are from the archive of the GFS (Global Forecast System) model runs. Figure 3.3C shows a skew-T diagram of an atmospheric sounding made in Schleswig, Germany, at 12 UTC on the 7th of December 2014. This sounding (extracted from the University of Wyoming website service) shows that the atmosphere was stable, and that precipitation was most likely falling. During this atmospheric state, precipitation is coming from Nimbostratus clouds. Precipitation from these type of clouds is falling at a relatively low rate compared to precipitation from unstable clouds such as Cumulonimbus.

3.2.2 Summer Case

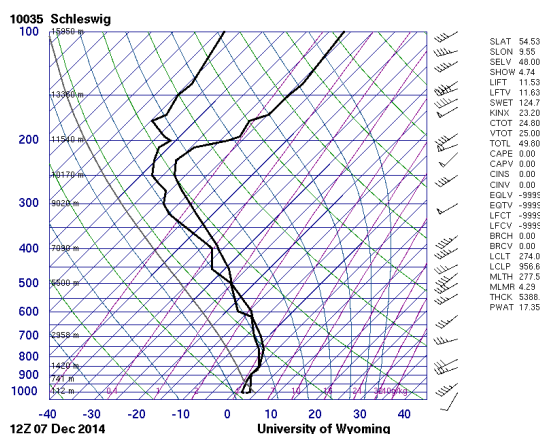
The synoptic situation on the 31st of May 2015 was dominated by low pressure systems located in the northern parts of Europe. A low pressure system moved in from the west, and along with it a frontal system with a warm and a cold front closely followed by each other. On the 31st of May at 18 UTC, the low pressure system was situated north of Great Britain and the frontal system was located close to Denmark and southern Sweden, as can be seen in Figure 3.4A. Northwest of the low pressure at centre of the frontal system,

³Figure 3.3A and 3.3B obtained at <http://www1.wetter3.de/Archiv/>, Figure 3.3C obtained at <http://weather.uwyo.edu/upperair/sounding.html>.



(A) Surface analysis at 18 UTC.

(B) Precipitation intensity at 18 UTC.



(C) Atmospheric sounding diagram from Schleswig (Germany) at 12 UTC.

FIGURE 3.3: Maps and diagrams describing the synoptic situation of Northern Europe on the 7th of December 2014³.

another low pressure system was located and between them an occluded front, which can also be seen in Figure 3.4A.

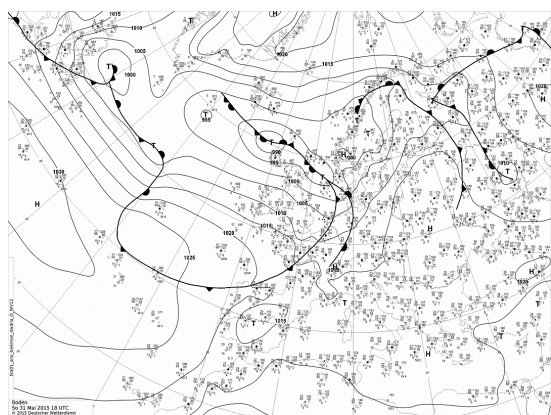
As the front approached Denmark and southern Sweden on the 31st of May, the wind changed from a westerly to a southerly direction. The air temperature in the morning of the 31st was 5-7°C in southern Sweden and 6-8°C in Denmark, and increased to 13-15°C over both land areas during the day. The air temperature over the sea areas was 9-11°C. At 18 UTC on the 31st of May, when the front was close to Denmark and southern Sweden, the wind was southerly with a speed of 5 m/s over the land areas, and westerly with a speed of 10 m/s over the sea-area east of Great Britain. The temperature had decreased to 10-12°C over land and remained the same as before over the sea.

After the front passage on the 1st of June, the flow was westerly over the area of study and had approximately the same wind speeds over the ocean and the land as during the passage.

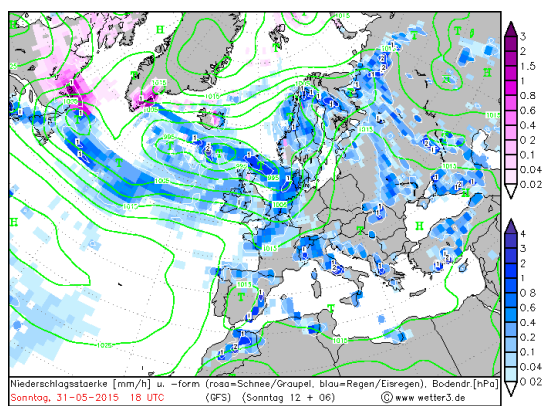
The frontal precipitation started falling over the North Sea, Denmark and southern Sweden around 18 UTC on the 31st of May, as can be seen in Figure 3.4B. During the

night on 1st of June the frontal zone moved north-west and covered most of Denmark and southern Sweden and a smaller part of the North Sea. The precipitation did no longer occur in the area in the morning of the 1st of June.

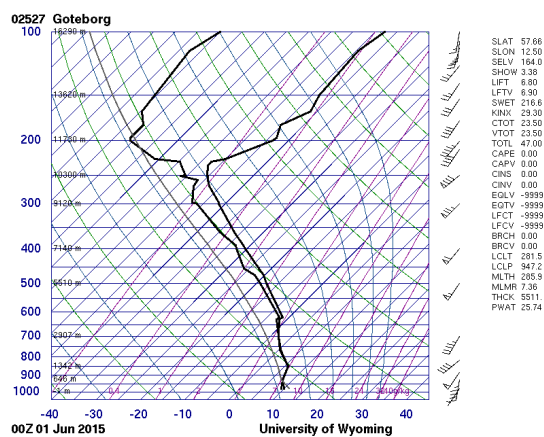
The values of air temperature, wind characteristics and precipitation mentioned above are from the archive of the GFS (Global Forecast System) model runs. The atmospheric sounding (extracted from the University of Wyoming website service) from Gothenburg, Sweden at 00 UTC on the 1st of June in Figure 3.4C shows a stable atmosphere and the precipitation is falling from Nimbostratus clouds and at a relatively low rate.



(A) Surface analysis at 18 UTC.



(B) Precipitation intensity at 18 UTC.



(C) Atmospheric sounding diagram from Gothenburg (Sweden) at 00 UTC.

FIGURE 3.4: Maps and diagrams describing the synoptic situation of Northern Europe on the 31st of May 2015 (Fig. A & B) and 1st of June 2015 (Fig. C)⁴.

⁴Figure 3.4A and 3.4B obtained at <http://www1.wetter3.de/Archiv/>, Figure 3.4C obtained at <http://weather.uwyo.edu/upperair/sounding.html>.

Chapter 4

Results and Discussion

4.1 Analysis for Winter Case

4.1.1 Short Wave Radiation

On the 7th of December 2014, the sunrise occurred at 07:30 UTC and the sunset at 14:30 UTC in Denmark, the centre of the area of study. During the few hours of sunlight, the sea salt aerosols showed an impact on the short wave radiation flux at the surface. When the difference in short wave radiation flux is averaged over the entire domain, the presence of sea salt aerosols lead to a decrease of less than 1 W/m^2 in radiation reaching the surface. However, the difference in short wave radiation flux varies greatly over the domain and in particular over the sea-ocean areas.

Figure 4.1 shows the variability in the difference between the two model runs (reference - excluding sea salt aerosols) on a diurnal cycle. After sunrise, the difference increases from a few W/m^2 to larger values ranging from -64 to $+76 \text{ W/m}^2$ at 09 UTC, and reaches its greatest value at 12 UTC, when it ranges from -188 to $+172 \text{ W/m}^2$. The difference in short wave radiation flux then decreases to smaller values ranging from -70 to $+64 \text{ W/m}^2$ at 15 UTC and continues to decrease rapidly to negligible values.

Figure 4.2 shows the difference field at 12 UTC on 7th of December 2014. In this figure it becomes clear that the sea salt aerosols have the largest and most visible impact over the sea-ocean surface (i.e. the area from where they originate) but the impact also propagates towards the coastal regions. The small average value of less than 1 W/m^2 arises due to the fact that the domain covers large areas with low concentrations of sea salt aerosols, which suppresses the large impact of these aerosols in some areas.

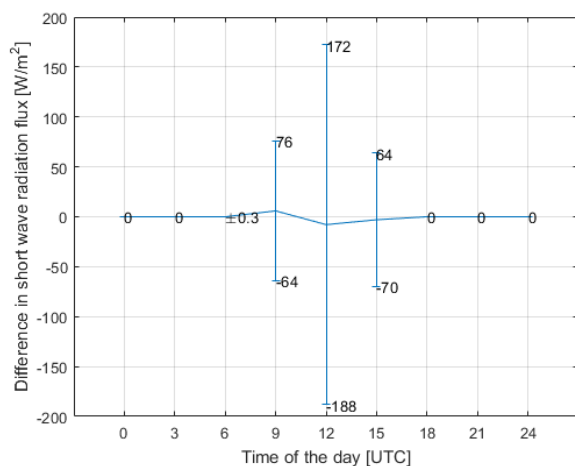


FIGURE 4.1: The difference in short wave radiation flux [W/m^2] at the surface, on a diurnal cycle, 7 Dec 2014.

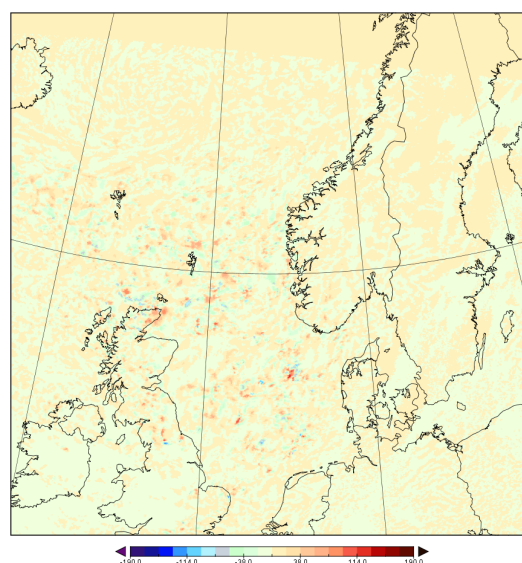


FIGURE 4.2: The difference in short wave radiation flux [W/m^2] at the surface on 7 Dec 2014, 12 UTC.

4.1.2 Air Temperature

Diurnal Cycle

The diurnal cycle of the variability in air temperature difference (reference - excluding sea salt aerosols) is plotted in Figure 4.3. The variability is smaller during night and early morning hours, varying between minimum values of -3.6 to -2.3 K and maximum values of $+1.6$ to $+2.6$ K. It then increases in morning hours with sun rising, starting at 09 UTC, up to values ranging from -4.8 to $+5.6$ K. During the daytime hours, the difference variability remains very similar, and it starts to decrease in late evening hours.

Figure 4.4 illustrates the evolution of the sea salt aerosol impact on selected times on a diurnal cycle. In this composite figure it can be seen that the area of impact increases and expands to several sectors on the diurnal cycle. The first signs of sea salt aerosol impact are observed at 06 UTC in the north-eastern part of domain, over the northern areas of the Norwegian Sea. These differences are relatively weak. At 09 UTC (Figure 4.4B), the area of impact has become substantially larger, expanding towards southern parts of the Norwegian Sea, Shetland and Faroe Islands. The differences are also larger. At 12 UTC, the area of impact has expanded westward, reaching the southern parts of Iceland. At the same time, the area has slowly propagated southward into the North Sea. The differences are even larger, especially over water surfaces. At 15 UTC (Figure 4.4C) the impact is observed in coastal regions of Norway and the UK. At the same time, the influence of the sea salt aerosols is observed in the central parts of the North Sea,

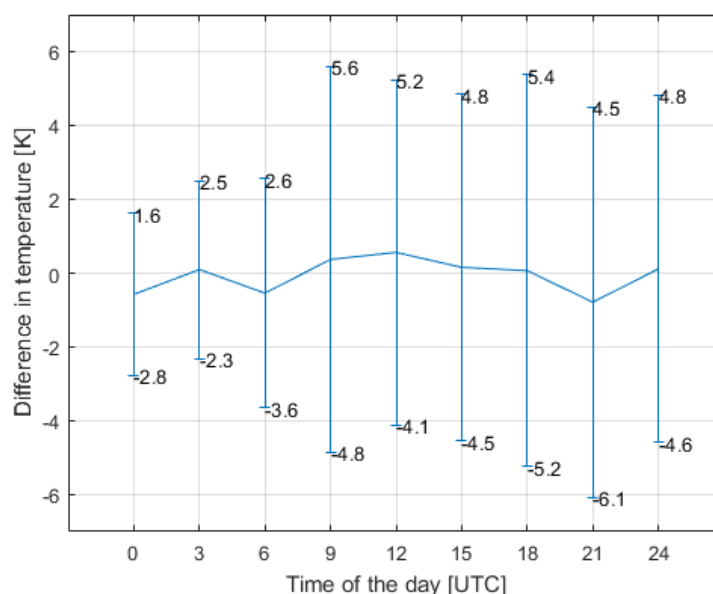


FIGURE 4.3: The difference in air temperature [K] at 2 m, on a diurnal cycle, 7 Dec 2014.

reaching the north-western parts of Denmark. At 18 UTC, the area of impact over the Norwegian Sea has evolved rapidly, and at the same time a larger impact is seen over coastal regions of the western parts of Denmark (Jutland Peninsula). At 21-24 UTC (Figure 4.4D), the impact is seen over the Skagerrak and Kattegat passages and on the coast of north-western Germany.

When comparing Figure 4.4C with Figure 3.3B in the methodology section, it can be seen that the largest effect from the sea salt aerosols is found in connection with the presence of the low pressure system located outside Norway's west coast. Towards the end of the forecast (Figure 4.4D), when the frontal system is moving over Denmark and southern Sweden, an impact on the air temperature over these land areas can be seen.

Vertical Variability

When looking at the sea salt aerosol impact on the air temperature at different levels in the atmosphere, the largest impact is found within the planetary boundary layer (PBL). The PBL is the atmospheric layer with height of up to approximately 1 km and higher, depending on time of the day and geographical location. In this layer the friction of the surface is important, and there is usually more mixing within this layer compared to the air aloft (free troposphere). Therefore, the aerosol concentration becomes larger in the PBL and the effect will be more visible.

Following analysis on a diurnal cycle, the hour of 18 UTC is selected to show variability within the layers of the atmosphere. For this case study, the aerosol effect

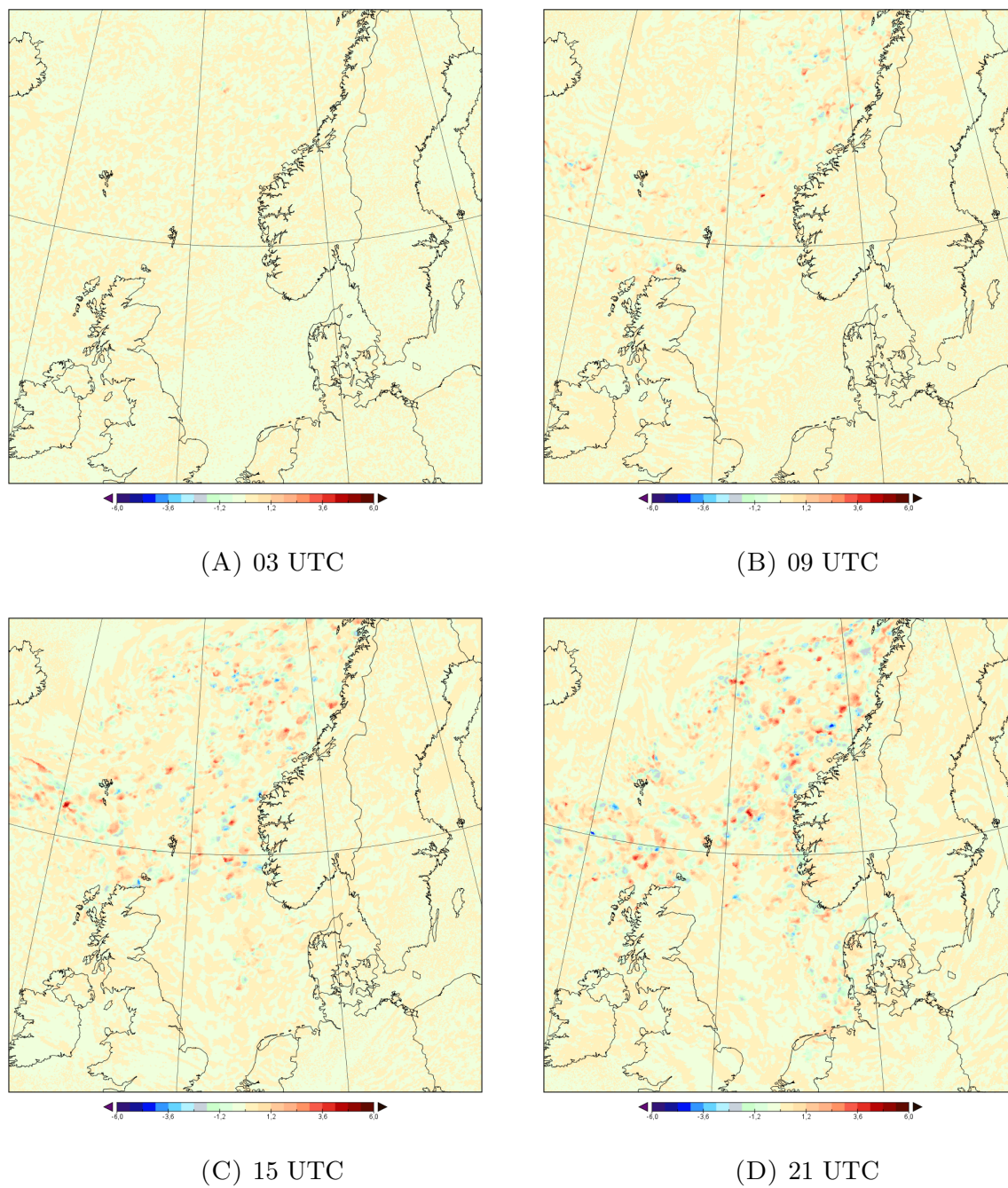


FIGURE 4.4: The air temperature difference [K] on a diurnal cycle at (A) 03, (B) 09, (C) 15, and (D) 21 UTC on 7 Dec 2014.

is strongly seen at the level of 1000 hPa (~ 100 m) as seen in Figure 4.5A. There is no significant impact on air temperature at the pressure levels of 850 hPa (~ 1.5 km) and 500 hPa (~ 5.5 km), as illustrated in Figures 4.5B and 4.5C. At the top of the troposphere, at 300 hPa (~ 9 km), the effect of the sea salt aerosols on the air temperature can be seen as well, as shown in Figure 4.5D. Moreover, the total area of aerosol impact is the largest in the lowest parts of the boundary layer compared to other layers of the troposphere.

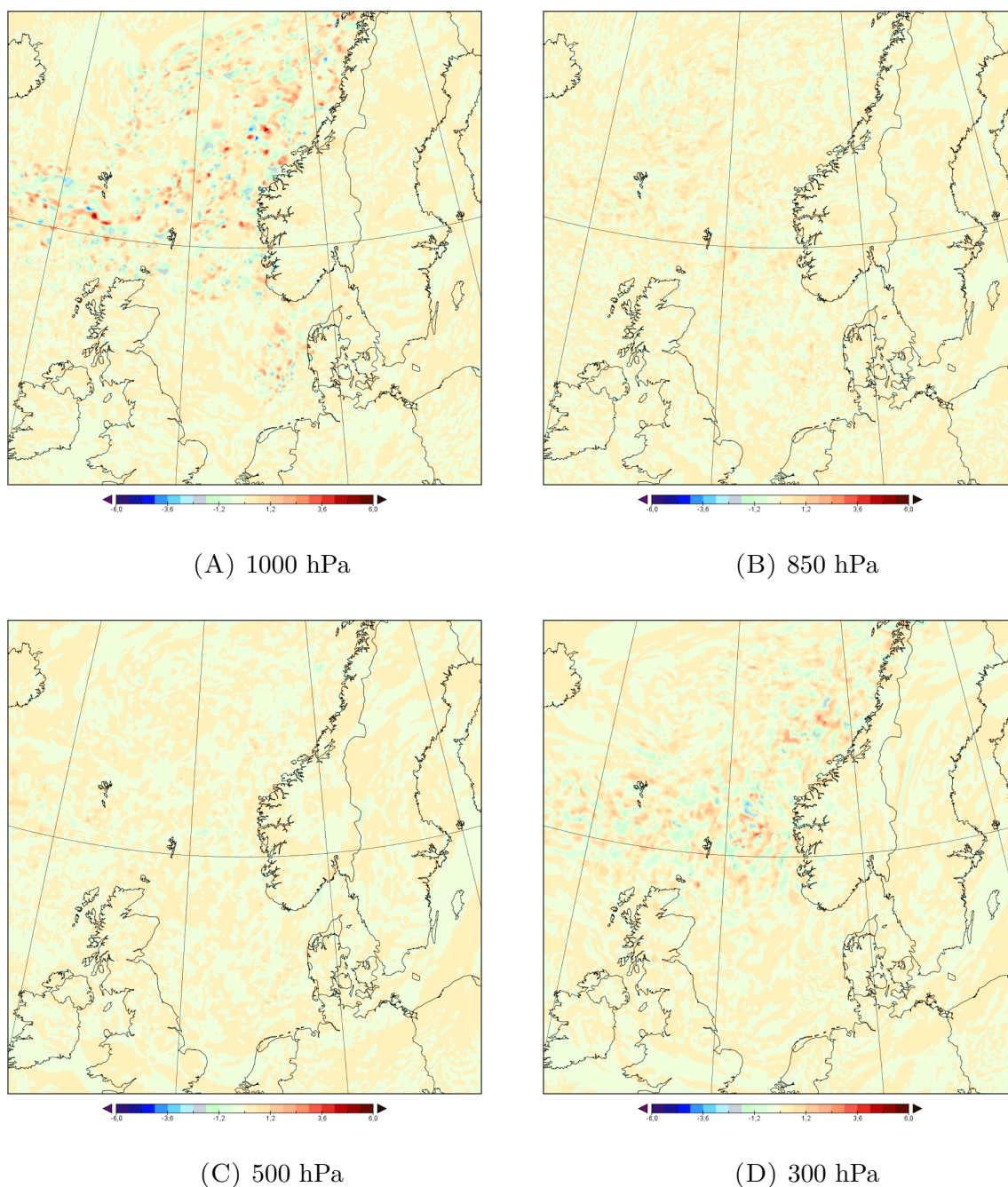


FIGURE 4.5: The air temperature difference [K] at pressure levels of (A) 1000, (B) 850, (C) 500 and (D) 300 hPa in the atmosphere on 7 Dec 2014, 18 UTC.

4.1.3 Relative Humidity

Diurnal cycle

The variability in the difference (reference - excluding sea salt aerosols) in relative humidity on a diurnal cycle is plotted in Figure 4.6. At 00 UTC, the difference in relative humidity varies between values of -23 and +12 %. During the night and until 09 UTC the variability gradually increases and the minimum values range from -35 to -30 % and the maximum values range from +29 to +41 %. The variability further increases at 12 UTC and remains very similar during the day and evening hours, with minimum values ranging from -49 to -43 % and maximum values ranging from +41 to +45 %.

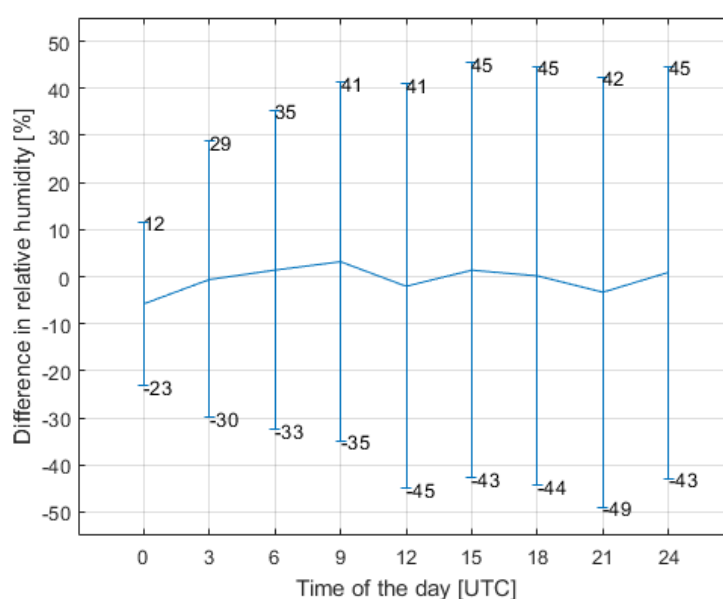


FIGURE 4.6: The difference in relative humidity [%] at 2 m, on a diurnal cycle, 7 Dec 2014.

In Figure 4.7, the evolution of the sea salt aerosol impact on relative humidity can be seen. The first aerosol impact is observed at 03 UTC (Figure 4.7A) in the northern parts of the Norwegian Sea. The differences are at this time relatively weak. At 06 UTC, the area of impact has increased towards the southern parts of the Norwegian Sea, the Faroe Islands, and the UK and shows slightly larger differences. At 09 UTC (Figure 4.7B) the area of impact has expanded westward, reaching southern Iceland, with increased differences. At 12 UTC, the aerosol impact is visible in the North Sea and covers larger parts of the Norwegian Sea. At 15 UTC (Figure 4.7C) the area of impact has extended further south-east, reaching the land area of southern Norway, and shows stronger differences over the Norwegian and North Seas. At 18 UTC, the area of impact, which is still expanding south-east, has reached the western parts of Denmark

(the Jutland Peninsula). At 21 UTC (Figure 4.7D) the area of impact has extended into the Skagerrak and Kattegat passages and reaches the west coast of Sweden. Further extension of the area shows the effect of aerosols on the west coast of the UK at 00 UTC, 8 December 2014.

When comparing Figure 4.7D with Figure 3.3A, the sea salt aerosol impact on relative humidity over Denmark can be seen to occur in connection to the cold front passing through the area. The impact over the Norwegian Sea, see Figure 4.7D, is linked with the low pressure system located outside the west coast of Norway, shown in Figure 3.3B.

Vertical Variability

For the analysis of sea salt aerosol impact on relative humidity within layers of the atmosphere, the hour of 18 UTC is chosen. The impact of sea salt aerosols is shown in Figure 4.8. The aerosol effect is clearly visible at the level of 1000 hPa (~ 100 m), as shown in Figure 4.8A. The area of impact increases rapidly with height and the largest area of impact is found at 850 hPa (~ 1.5 km), leading to impact over land surfaces of the Scandinavian and Jutland Peninsulas, as well as over sea-ocean areas. The differences are also larger in absolute values, which can be seen in Figure 4.8B. The strongest differences are seen at 500 hPa (~ 5.5 km), as shown in Figure 4.8C. The impact then decreases very rapidly with height, both the absolute value of the differences and the size of total area of impact. A small impact of sea salt aerosols can be seen in Figure 4.8D, which shows the 300 hPa level (~ 9 km). Such rapid decrease depend on vertical extension of cloud cover within the troposphere.

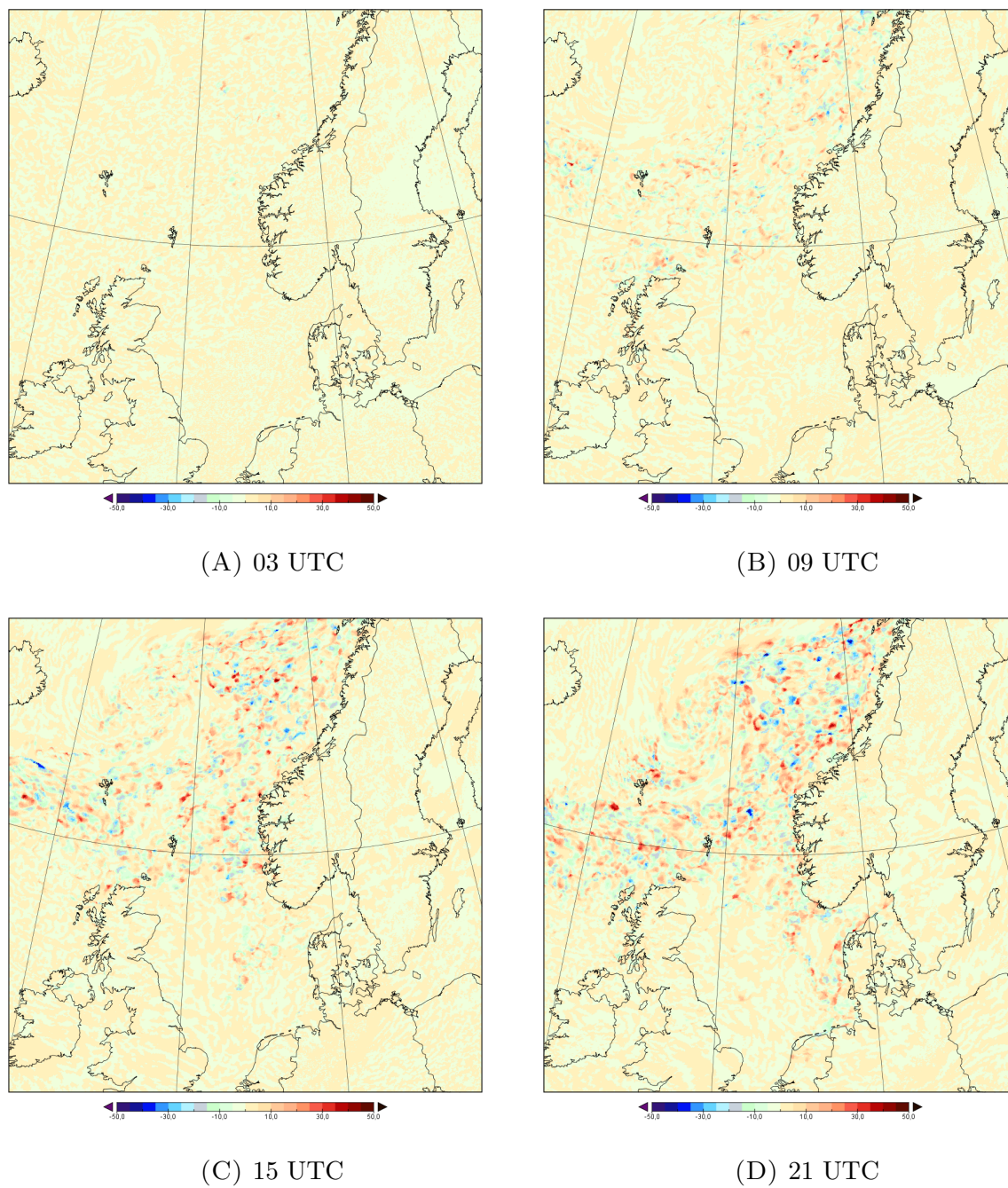


FIGURE 4.7: The difference in relative humidity [%] at (A) 03, (B) 09, (C) 15, (D) 21 UTC, 7 Dec 2014.

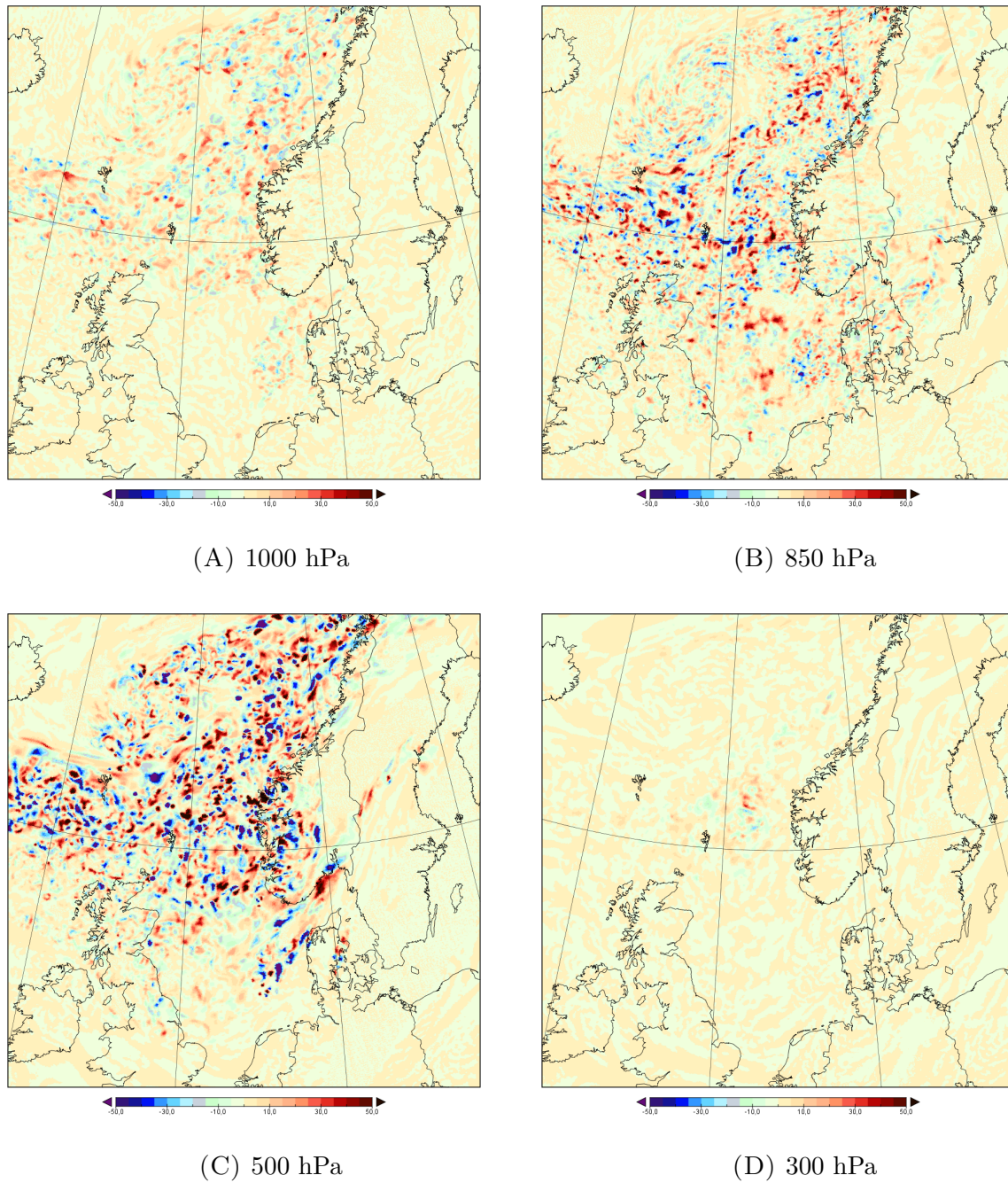


FIGURE 4.8: The difference in relative humidity [%] at pressure levels of (A) 1000, (B) 850, (C) 500 and (D) 300 hPa in the atmosphere on 7 Dec 2014, 18 UTC.

4.2 Analysis for Summer Case

4.2.1 Short Wave Radiation

On the 31st of May 2015, the sunrise occurred at 02:35 UTC and the sunset at 19:40 UTC in Denmark. In Figure 4.9, it can be seen that the sea salt aerosols had an impact on short wave radiation flux during the entire diurnal cycle, also during the hours of no sunlight in Denmark. This is because the domain covers areas with the midnight sun, meaning that the sun is above the horizon all day in these areas. The aerosol impact is the smallest during the night hours with values ranging between -11 and $+13$ W/m^2 , and it rapidly increases and reaches its maximum value at 9-12 UTC when the minimum values range from -671 to -631 W/m^2 and the maximum values range between $+541$ to $+629$ W/m^2 . After 12 UTC, the impact decreases fast to values ranging from -14 and $+15$ W/m^2 at 24 UTC.

Figure 4.10 shows the difference field (reference - excluding sea salt aerosols) in short wave radiation flux at 12 UTC on the 31st of May 2015. The largest impact is found south and east of Iceland, and in the southern part of the Baltic Sea. A small area of impact is also visible over land in the southern part of Sweden.

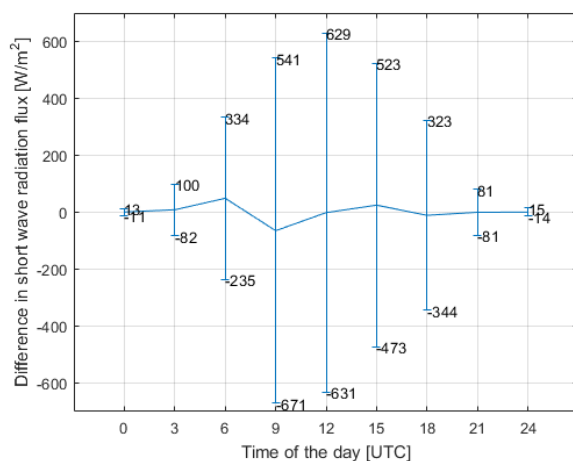


FIGURE 4.9: The difference in short wave radiation flux [W/m^2] at the surface, on a diurnal cycle, 31 May 2015.

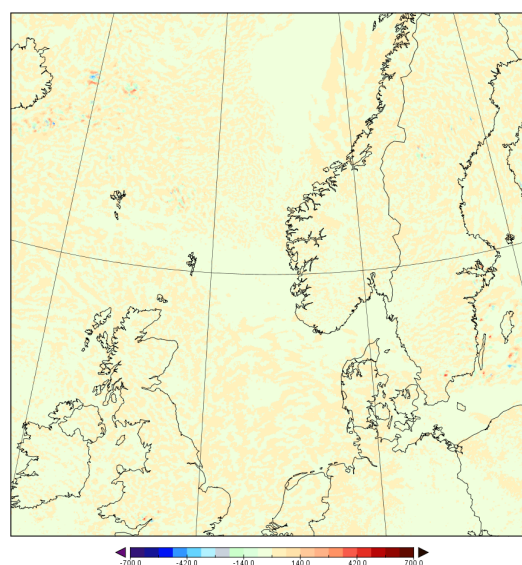


FIGURE 4.10: The difference in short wave radiation flux [W/m^2] at the surface on 31 May 2015, 12 UTC.

4.2.2 Air Temperature

Diurnal Cycle

The variability in air temperature difference (reference - excluding sea salt aerosols) on a diurnal cycle is plotted in Figure 4.11. This figure shows that the variability ranges from -2.1 to +3.8 K at 00 UTC, and increases and reaches its maximum variability at 03 UTC, ranging from -5.3 to +3.1 K. The variability then decreases during the day with minimum values ranging between -4.3 and -2.0 K and maximum values ranging between +1.8 and 3.6 K, during 06-21 UTC. Towards the end of this time interval the variability increases and at 24 UTC reaches values ranging from -4.6 to +3.7.

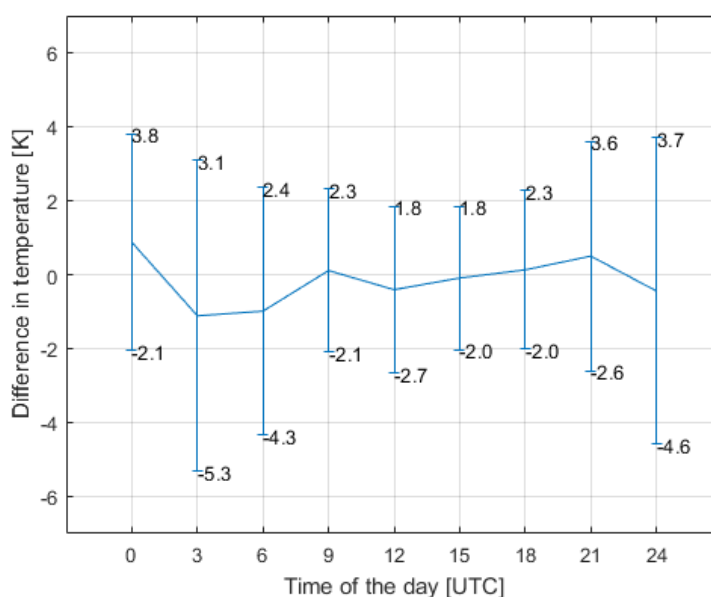


FIGURE 4.11: The difference in temperature [K] at 2 m, on a diurnal cycle, 31 May 2015.

In Figure 4.12, the evolution of the sea salt aerosol impact on air temperature is visualised for selected UTC times. The first impact is observed at 09 UTC (Figure 4.12B) and occurs over land in the south-eastern part of Sweden. The impact covers a small area and is relatively weak. At 12 UTC, this area of impact has decreased and a new area of impact has arisen in the middle of Sweden. At 15 UTC (Figure 4.12C) the impact in south-eastern Sweden is no longer visible. However the area of impact in mid and northern Sweden has expanded north-eastward. An area of impact has appeared in Finland. At 18 UTC, a stronger difference in northern Norway and Sweden is observed, the impact does however cover a smaller area than before. At 21 UTC (Figure 4.12D) the area of impact in this region has made a cyclonic (anti-clockwise) movement, meaning that parts of the impact is shifted north-west and parts of it is shifted south-east. An area of impact is

also observed in the northern part of the Baltic Sea and over the UK and the sea-ocean area north of the UK. At 24 UTC, the area of impact in Sweden has expanded south- and eastward and a more pronounced impact is seen over the UK and in the Baltic Sea.

The sea salt aerosol impact in Sweden and Norway, which can be seen in Figure 4.12D is found in connection with the low pressure system in the area, see Figure 3.4A. The impact outside the UK is also found to be linked to a frontal system, as seen when these two figures are compared.

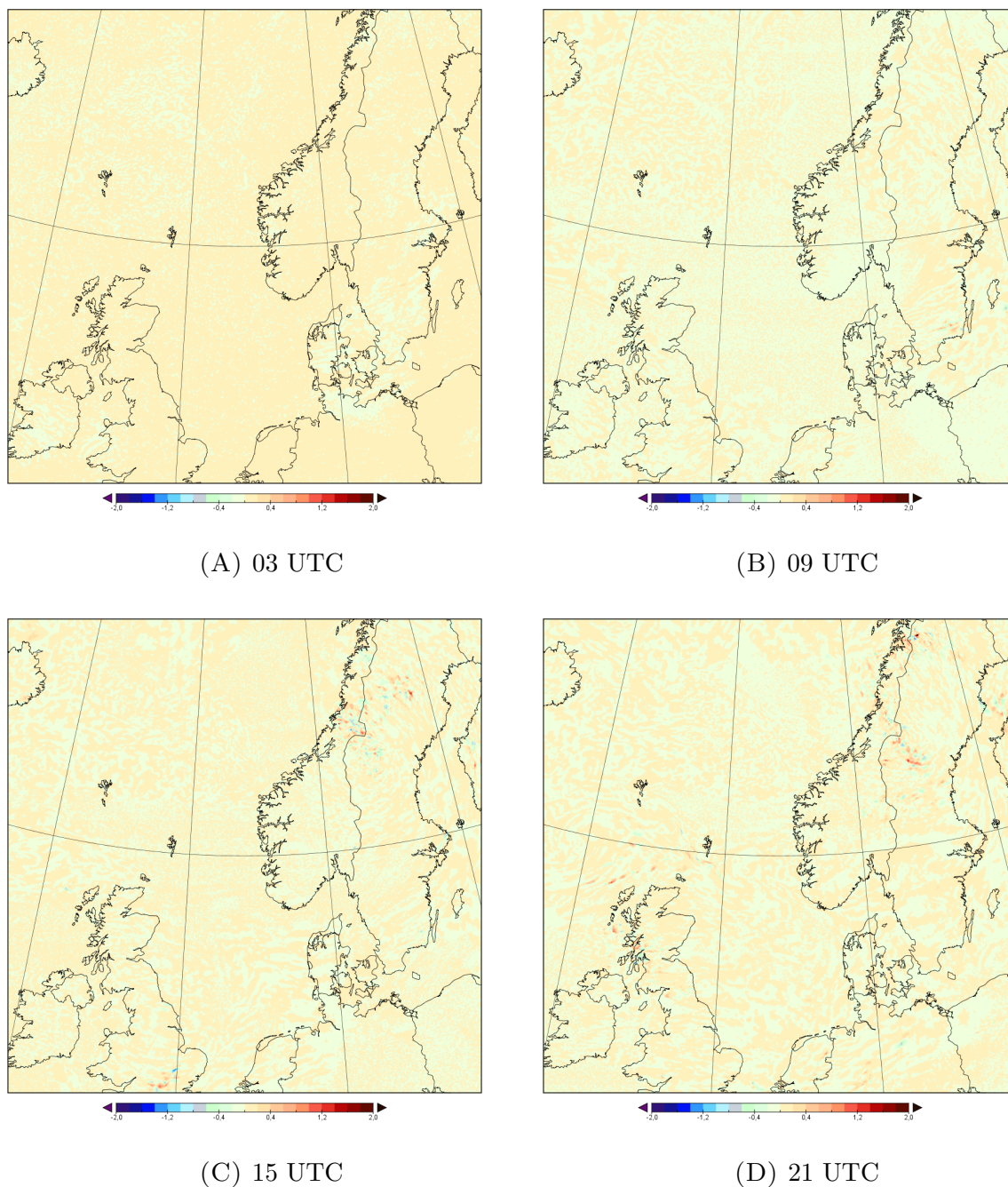


FIGURE 4.12: The air temperature difference [K] on a diurnal cycle at (A) 03, (B) 09, (C) 15, and (D) 21 UTC on 31 May 2015.

Vertical Variability

The sea salt aerosol impact on air temperature in levels of the atmosphere is investigated for the hour of 18 UTC. The largest differences are observed at the level of 1000 hPa (\sim 100 m) but this area of impact covers only a small geographical area, as seen in Figure 4.13A. At 850 hPa (\sim 1.5 km), the impact is not observed to be as strong but covers a larger area, as shown in Figure 4.13B. Further up in the atmosphere, at the levels of 500-300 hPa, only a weak impact over a small area can be observed, see Figure 4.13C and 4.13D. In summer, the PBL has a larger vertical extension and can reach heights of 1.5 km and above. The characteristics of the PBL could be the reason for a stronger sea salt aerosol impact at 1000 hPa and 850 hPa, compared to higher levels.

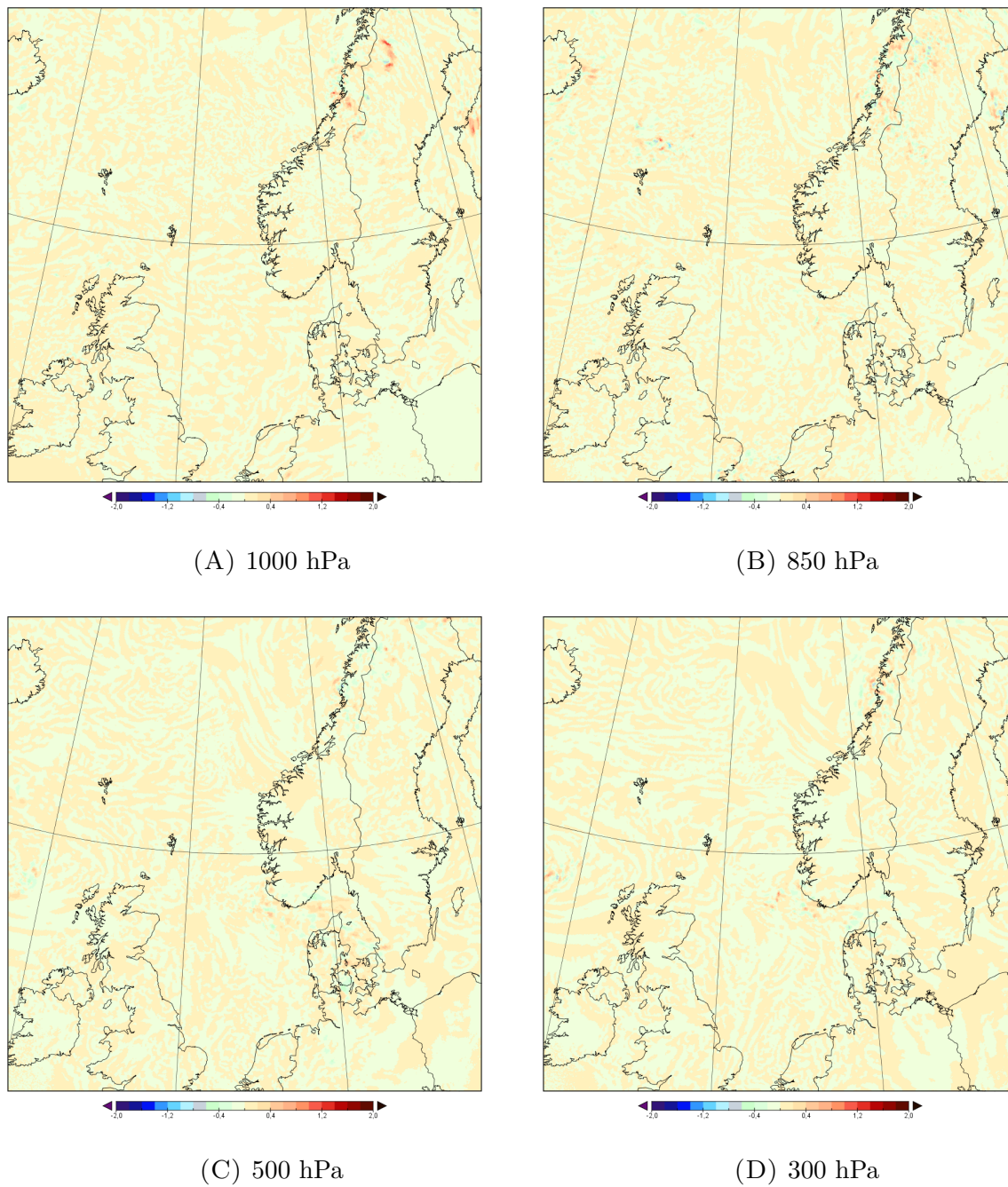


FIGURE 4.13: The air temperature difference [K] at pressure levels of (A) 1000, (B) 850, (C) 500 and (D) 300 hPa in the atmosphere on 31 May 2015, 18 UTC.

4.2.3 Relative Humidity

Diurnal Cycle

In Figure 4.14, the variability in relative humidity difference (reference - excluding sea salt aerosols) is plotted. The smallest variability is observed at 00 UTC and ranges from -11 to +11 %. It increases slightly during the night and the minimum values of the difference range between -15 to -13 % and the maximum values range from +17 to +22 %, between the hours of 03-12 UTC. The variability further increases to ranging between -28 to +19 % at 15 UTC. The highest variability in the difference occurs at 18 UTC when the values range between -23 to +29 %. Between 21-24 UTC the variability has decreased and the minimum values range between -18 and -22 % and the maximum values between +18 to +21 %.

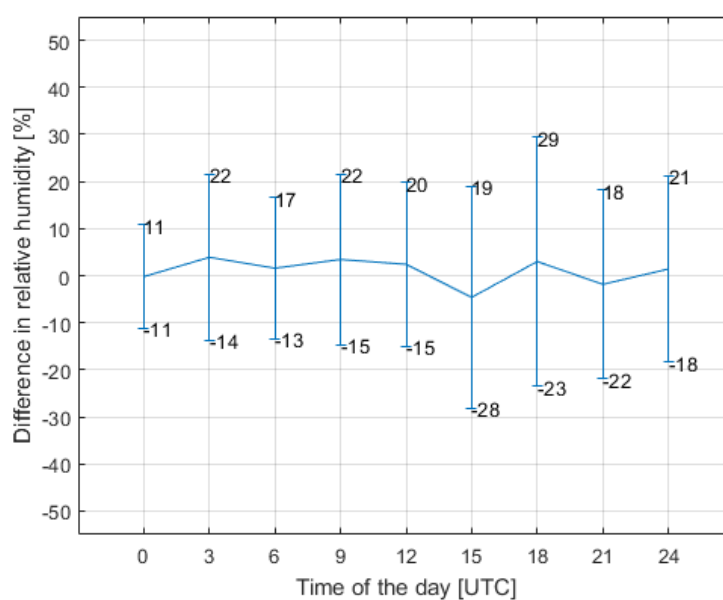
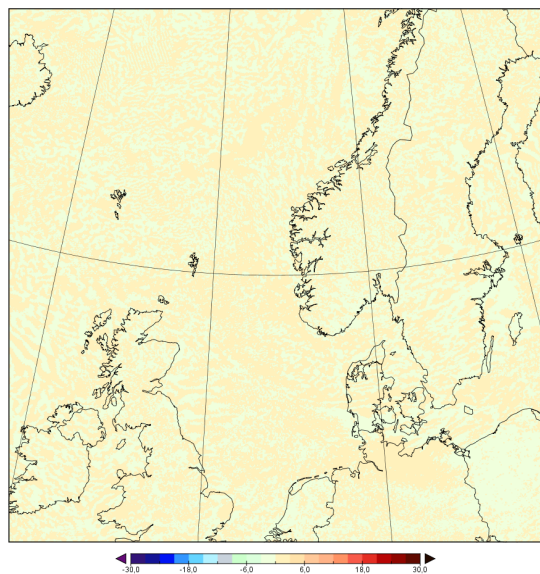


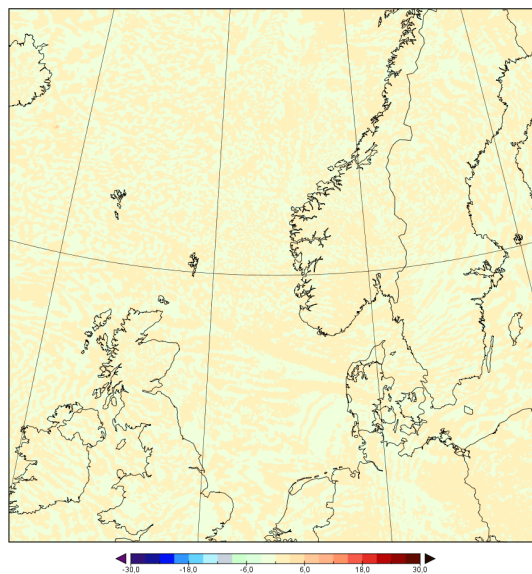
FIGURE 4.14: The difference in relative humidity [%] at 2 m, on a diurnal cycle, 31 May 2015.

Figure 4.15 illustrates the sea salt aerosol impact on relative humidity for selected times of the day. The first impact is observed at 15 UTC (Figure 4.15C), covering a small area in the northern part of Sweden and Norway. At 18 UTC, the area of impact has propagated north-eastward, but is not expanded. At 21 UTC (Figure 4.15D), the area of impact has propagated westward and is located on the west coast of Norway. An area of impact is also observed in the northern part of the Baltic Sea and over the UK and the sea-ocean area north of the UK. At 24 UTC the area of impact outside Norway has moved further west. The area of impact over the UK shows stronger differences and covers a larger area. The area of impact in the Baltic Sea is no longer observed. Overall, the difference fields for relative humidity show only small differences on the diurnal cycle.

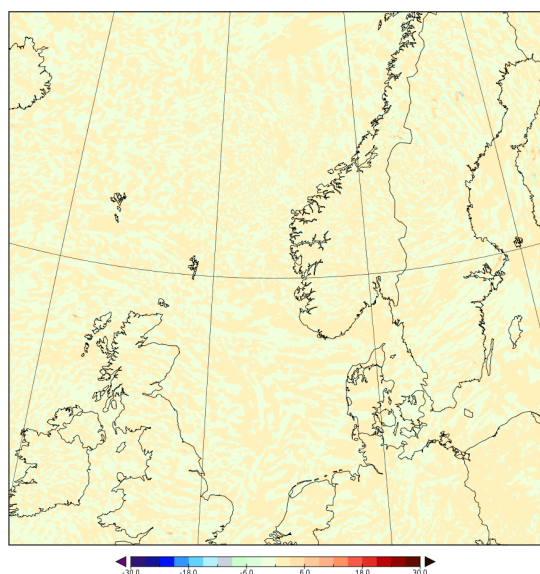
Comparing Figure 4.15D with Figure 3.4A, it can be seen that there is an occluded front located along Norway's coast to which the sea salt impact is linked. The area of aerosol impact outside the UK also occurs in connection with a frontal system in the area.



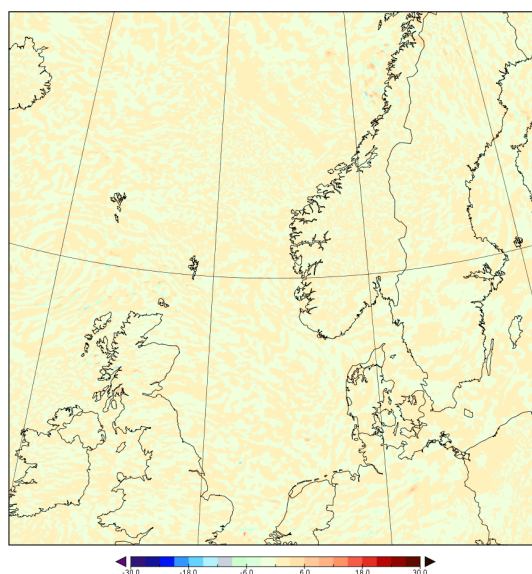
(A) 03 UTC



(B) 09 UTC



(C) 15 UTC



(D) 21 UTC

FIGURE 4.15: The difference in relative humidity [%] at (A) 03, (B) 09, (C) 15, (D) 21 UTC

Vertical Variability

For the analysis of sea salt aerosol impact on relative humidity at different levels in the atmosphere, the hour of 18 UTC is chosen. Figure 4.16 shows the vertical variability at this hour. In Figure 4.16A, it can be seen that a small area of impact is visible at the 1000 hPa ($\sim 100\text{m}$) level. The area of impact increases with height and covers several parts of the domain at the 850 hPa ($\sim 1.5\text{ km}$) level, as shown in Figure 4.16B. The most pronounced impact is found at 500 hPa ($\sim 5.5\text{ km}$), which occurs over northern Sweden, north-west of the UK, over Denmark and southern Sweden, and over parts of the North Sea, as can be seen in Figure 4.16C. The area of impact decreases towards the top of the troposphere and shows an impact only over Denmark, the Skagerrak and Kattegat passages and parts of the North Sea, at the 300 hPa level ($\sim 9\text{ km}$), which is shown in Figure 4.16D.

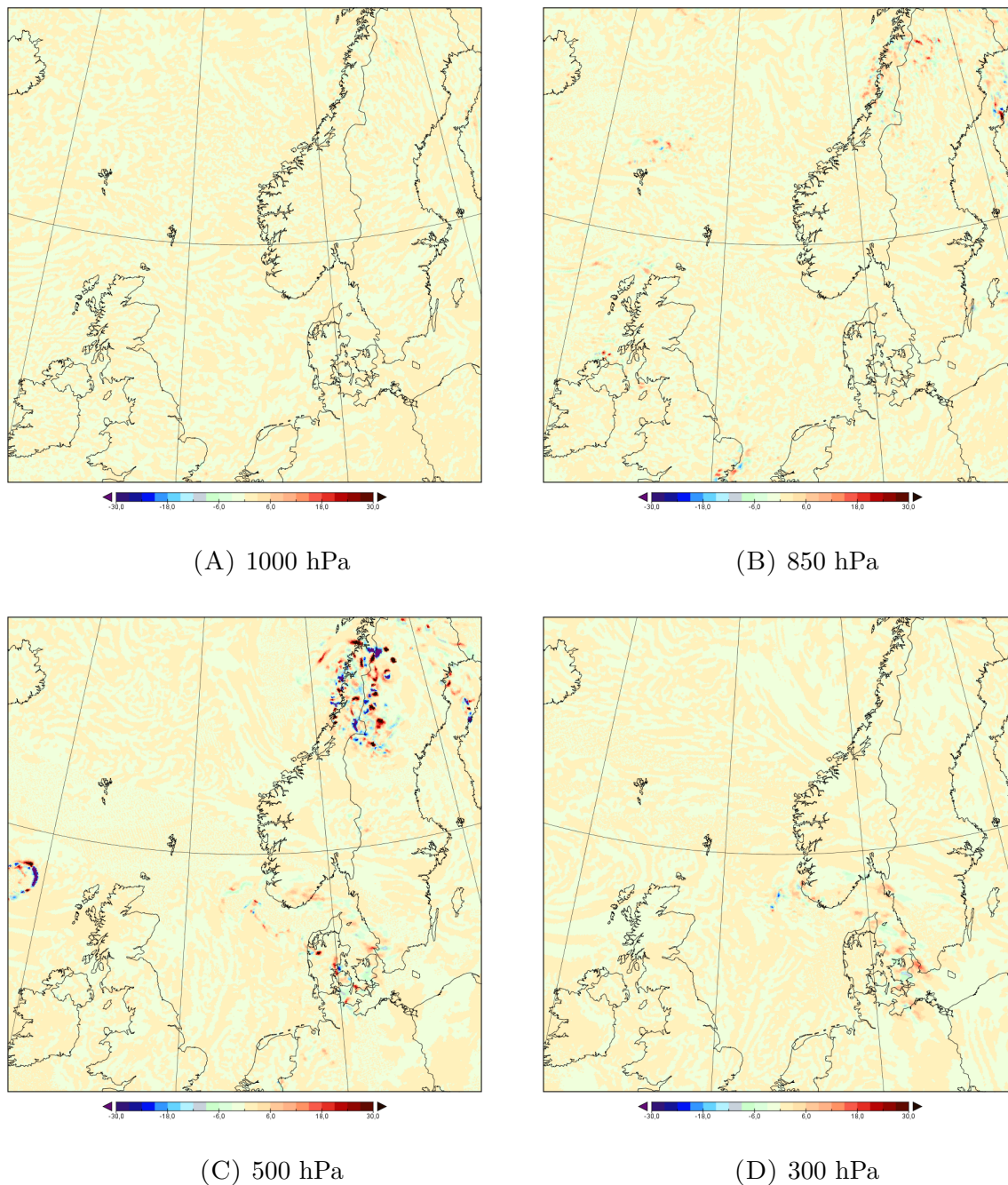


FIGURE 4.16: The difference in relative humidity [%] at pressure levels of (A) 1000, (B) 850, (C) 500 and (D) 300 hPa in the atmosphere on 31 May 2015, 18 UTC.

Chapter 5

Conclusion and Outlook

The main aim of this study was to investigate the impact of sea salt aerosols on numerical weather prediction during low precipitation events. At first, two dates (also referred to as cases), one in winter (7 Dec 2014) and one in summer (31 May 2015) were selected and the meteorological situations of these dates were analysed and described using surface maps and sounding data. For the two cases, the HARMONIE NWP model was configured at the ECMWF HPC for a domain covering the northern European area. Model runs were then made (for the full day with 6 hour spin-up) with and without sea salt aerosols. The modelling results were evaluated for changes in short wave radiation, air temperature and relative humidity on a diurnal cycle at the surface and at selected vertical levels within the atmosphere.

In the winter case study (7 Dec 2014), it was found that the variability in short wave radiation flux was the largest at 12 UTC ranging from -188 to $+172$ W/m^2 and was smaller at dawn and dusk. The most visible difference occurred over the sea-ocean areas, where sea salt aerosols originate from. The variability in air temperature on a diurnal cycle was largest during daytime ranging from -4.8 to $+5.6$ K and more than half the magnitude smaller during night and morning hours. The impact of sea salt aerosols on air temperature was found in connection to an evolving low pressure system in the Norwegian Sea. Vertically, the largest impact was seen at 1000 hPa (~ 100 m) compared to other levels, hence the total area of aerosol impact was largest in the lowest parts of the boundary layer compared to other levels of the troposphere. Studying the variability in relative humidity on a diurnal cycle showed that it gradually increased in the morning hours and was largest during the daytime, ranging from -49 to $+45$ %, with similar values the remaining hours of the day. Similarly to air temperature, the sea salt aerosol impact on relative humidity occurred over the same geographical areas, as well as being linked with the same low pressure system. However, vertically, the variability in relative humidity was more pronounced at the 850-500 hPa layer with the strongest changes at 500 hPa (~ 5.5 km).

In the summer case study (31 May 2015), it was found that the variability in short wave radiation flux increased during morning hours, reaching its maximum value at 12 UTC, ranging from -631 to $+629$ W/m^2 , and gradually decreased towards the end of the diurnal cycle. When looking at the air temperature on the diurnal cycle, the largest variability was found during night time with maximum value at 03 UTC, ranging from -5.3 to $+3.1$ K. During the daytime hours (06-21 UTC) the variability was found to be

lower. The areas of impact on air temperature were found to be linked to two low pressure systems located in the area of study. The vertical variability in air temperature was the largest in the PBL, compared to higher levels. The highest variability in the difference in relative humidity was found at 18 UTC and it ranged from -23 to +29 %. For the other hours on the diurnal cycle, the variability was slightly lower. The difference fields of the relative humidity on the diurnal cycle showed only small impacts of sea salt aerosols. As in the case of air temperature, the impact on relative humidity occurred in connection with the two low pressure systems. In the vertical, the impact on relative humidity was found to increase with height up to the 500 hPa (~ 5.5 km) level, where the strongest impact was found.

In summary, a sea salt aerosol impact over the model domain was found for all meteorological parameters during both cases. In winter, the impact mainly occurred over sea-ocean areas, where the low pressure system was located. In the summer case, two low pressure systems were located in the area of study, one over the sea-ocean area and one over land, and the impact occurred in these two regions. The impact on air temperature at levels in the atmosphere was found to be the strongest in the PBL and the impact on relative humidity was found to be strongest at the levels of 850-500 hPa.

The impact on air temperature and relative humidity was stronger during the winter case than in the summer case. Low pressure systems tend to be deeper in the winter compared to the summer. Deeper low pressure systems lead to higher wind speeds, causing more sea salt aerosols to be produced which is the reason for a stronger impact on air temperature and relative humidity during winter. Regarding short wave radiation flux, the impact was found to be stronger in the summer. The few hours of sunlight during winter is the reason for a lower impact on short wave radiation flux during winter compared to summer.

This study showed importance of sea salt aerosol inclusion in numerical weather prediction. These aerosols are important for precipitation formation in both winter and summer conditions. It should be noted that aerosols might have an influence on other meteorological parameters, such as cloud cover, wind characteristics, turbulent kinetic energy, etc. So, for future studies, evaluation of these and other parameters would be important for other meteorological situations, other times of the year, and other geographical regions. In addition, including assimilation of ground-based and satellite aerosol data on operational scale, improving parametrisations of aerosol processes in the models, including potential sources and regions of aerosol emissions, etc. would be desirable. Such studies could lead to improvement of operational weather forecasts.

Bibliography

- Andreae, M. O., Jones, C. D., and Cox, P. M. Strong present-day aerosol cooling implies a hot future. *Nature*, 435(7046):1187–1190, 2005.
- Boucher, O., Randall, D., Artaxo, P., Bretherton, C., Feingold, G., Forster, P., Kerminen, V.-M., Kondo, Y., Liao, H., Lohmann, U., Rasch, P., Satheesh, S., Sherwood, S., Stevens, B., and Zhang, X. *Clouds and Aerosols*, chapter 7, pages 571–658. Cambridge University Press, Cambridge, United Kingdom and New York, NY, USA, 2013.
- Charlson, R. J., Schwartz, S., Hales, J., Cess, R. D., COAKLEY, j. J., Hansen, J., and Hofmann, D. Climate forcing by anthropogenic aerosols. *Science*, 255(5043):423–430, 1992.
- Driesenaar, T. General description of the harmonie model, 2009. <http://hirlam.org/index.php/hirlam-programme-53/general-model-description/mesoscale-harmonie>, accessed 1 March 2016.
- Driesenaar, T. Welcome to hirlam! about the hirlam programme, 2010. <http://hirlam.org/index.php/hirlam-programme-53/welcome-to-hirlam>, accessed 1 March 2016.
- Haywood, J. and Boucher, O. Estimates of the direct and indirect radiative forcing due to tropospheric aerosols: A review. *Reviews of geophysics*, 38(4):513–543, 2000.
- Kalnay, E. *Atmospheric modeling, data assimilation and predictability*. Cambridge university press, 2003.
- Krishnamurti, T. N., Bedi, H., Hardiker, V., and Watson-Ramaswamy, L. *An introduction to global spectral modeling*, volume 35. Springer Science & Business Media, 2006.
- Kristensson, A. and Martinsson, B. A beginner’s guide to atmospheric aerosol particles, compendium distributed in the unit Atmospheric Environmental Chemistry at Lund University, Sweden on 18 November. 2015.
- Palamarchuk, I., Ivanov, S., Ruban, I., and Pavlova, H. Influence of aerosols on atmospheric variables in the harmonie model. *Atmospheric Research*, 169:539–546, 2016.
- Palamarchuk, J., Ivanov, S., Kaas, E., Nuterman, R., and Mahura, A. Harmonie case study: Aerosol impact on atmospheric meso-scale circulation for nordic countries., 2015.
- Seifert, A., Köhler, C., and Beheng, K. Aerosol-cloud-precipitation effects over germany as simulated by a convective-scale numerical weather prediction model. *Atmos. Chem. Phys*, 12(2):709–725, 2012.

-
- Seity, Y., Brousseau, P., Malardel, S., Hello, G., Bénard, P., Bouttier, F., Lac, C., and Masson, V. The arome-france convective-scale operational model. *Monthly Weather Review*, 139(3):976–991, 2011.
- Toll, V., Reis, K., Ots, R., Kaasik, M., Männik, A., Prank, M., and Sofiev, M. Silam and macc reanalysis aerosol data used for simulating the aerosol direct radiative effect with the nwp model harmonie for summer 2010 wildfire case in russia. *Atmospheric Environment*, 121:75–85, 2015.
- Toll, V., Gleeson, E., Nielsen, K., Männik, A., Masek, J., Rontu, L., and Post, P. Impacts of the direct radiative effect of aerosols in numerical weather prediction over europe using the aladin-hirlam nwp system. *Atmospheric Research*, 2016.